URANIUM PYROPHORICITY PHENOMENA AND PREDICTION

Martin G. Plys, Michael Epstein, and Boro Malinovic
Fauske & Associates, Inc.
16W070 W. 83rd St.
Burr Ridge, Illinois 60521 USA
(630) 323-8750
Plys@Fauske.com

ABSTRACT

We have compiled a topical reference on the phenomena, experiences, experiments, and prediction of uranium pyrophoricity for the Hanford Spent Nuclear Fuel Project (SNFP) with specific applications to SNFP process and situations. The purpose of the compilation is to create a reference to integrate and preserve this knowledge. Decades ago, uranium and zirconium fires were commonplace at Atomic Energy Commission facilities, and good documentation of experiences is surprisingly sparse. Today, these phenomena are important to site remediation and analysis of packaging, transportation, and processing of unirradiated metal scrap and spent nuclear fuel. Our document, bearing the same title as this paper, will soon be available in the Hanford document system [Plys, et al., 2000]. This paper explains general content of our topical reference and provides examples useful throughout the DOE complex. Moreover, the methods described here can be applied to analysis of potentially pyrophoric plutonium, metal, or metal hydride compounds provided that kinetic data are available. A key feature of this paper is a set of straightforward equations and values that are immediately applicable to safety analysis.
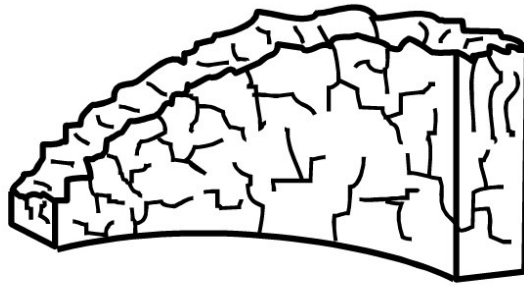
1.0 BACKGROUND AND PURPOSE

The phenomenon of pyrophoricity has been studied for chemical process safety and its mathematical formulation, ignition theory, is well established. We have applied ignition theory to experiments conducted with uranium powders and foils using recently available kinetic rate laws, and found that results can be explained and understood, where before these results were not quantified and were on occasion misinterpreted [Epstein, et al., 1996]. Also, documented experience suggests that the rate law for metal oxidation in air is applicable to uranium hydride, as will be shown below. Validation of the method appears in the reference and will not be repeated here. Instead, a brief explanation of the stationary, constant reaction rate theory will be given with example application, to convey the fundamental ideas. This technique is sufficiently accurate for safety analysis purposes because often system characteristics such as metal fraction or thermal conductivity are imprecisely known and this accuracy is demonstrated here. We also recommend this technique because it can be readily applied to more complex problems, as will be shown later. The purpose of this paper is to explain the recommended analysis procedure and its application in progressively more complex circumstances.

2.0   PRESENTLY RECOMMENDED TECHNIQUE

2.1   Equations and Approximations

Consider a reactive, porous medium of uranium metal or hydride, with internal resistance to heat transfer, rejecting heat to a known surface boundary temperature. This may be a powder or particle bed, or a metal fuel scrap piece with internally connected porosity and possibly hydriding in the cracks, Figure 1. The reaction rate of uranium metal with air, water, or water vapor is represented by an Arrhenius expression whose coefficient and activation energy depend upon the choice of oxidizer up to about 300°C [Ritchie, 1981; Pearce, 1989; and McGillivray, et al., 1994]. Due to internal heat generation and internal resistance to heat transfer, there is a temperature gradient across the reacting medium. Therefore the reaction rate varies across the medium. An exact form for the temperature profile and boundary temperature that leads to runaway reaction can be found, which constitutes the classical analysis of [Frank-Kamenetskii, 1969]. Here we follow the constant reaction rate method introduced by [Thomas and Bowes, 1961], and evaluate the reaction rate at a single temperature.

Figure 1: Declad, Cracked, Internally Hydrided Scrap Piece.

BM986103.CDR 6-30-98

Assuming a constant internal heat generation and a significant temperature gradient in only one direction, the difference between the maximum temperature in the medium and its boundary temperature is given by the familiar quadratic relation:

$$T_m - T_\infty \quad = \quad \frac{Q_v\,L^2}{2\,k} \tag{1}$$

where $Q_v \quad = \quad A_v\,\Delta H\,k_o\,e^{-T_E/T_m}$ (2)a

$A_v \quad = \quad \dfrac{6\,(1-\phi)}{d_p}$ (2)b

$T_m \quad = \quad$ Maximum temperature, K,

$T_\infty \quad = \quad$ Boundary temperature, K,

$L \quad = \quad$ Conduction distance, m,

$k \quad = \quad$ Thermal conductivity, W/m-K,

$A_v \quad = \quad$ Area per unit volume, m^{-1},

ϕ = Porosity (non-fuel volume fraction),

d_p = Average particle diameter, m,

ΔH = Heat of reaction, J/kg

k_o = Arrhenius coefficient, kg/m^2-s, and

T_E = Normalized activation energy, K.

Note that the maximum temperature of the medium is used to evaluate the reaction rate. The area per unit volume is the reactive surface area, and its evaluation must consider surface area due to internal porosity, metal fraction, or hydride inclusions. Also, the conduction distance is defined from the outer boundary to an insulating boundary, which is for example the bottom of a powder bed or the middle of a scrap piece exposed to oxidant on both sides. The Frank-Kamenetskii approximation is made to the heat of reaction, so that

$$e^{-T_E/T_m} \qquad e^{-T_r} e^{T_r \theta} \tag{3}$$

$$T_r = \frac{T_E}{T_\infty} \tag{4}$$

$$\theta = \frac{(T_m - T_\infty)}{T_\infty} \tag{5}$$

When the above equations are combined, all terms containing the maximum temperature T_m may be isolated on one side, and terms which are constant for a given set of properties and boundary conditions may be isolated on the other:

$$T_r \theta e^{-T_r \theta + 1} = \frac{A_v L^2 k_o \Delta H T_r}{2 k T_{dk} \exp(T_r - 1)} \equiv B \tag{6}$$

Thus, the value of the constant B determines the value of the maximum temperature T_m. Inspection of the left-hand side function reveals that a maximum is achieved when the product $T_r \theta = 1$, which occurs for a value of B = 1. Therefore there are no physical solutions of the equation for B > 1, and there are two solutions for T_m for values of B < 1. Only those solutions for T_m less than the value which maximizes B are physically stable steady-state temperatures. Therefore the critical value B = 1 divides stable, steady-state temperature solutions in the reacting medium from those that are unstable; the form of B was chosen so that the critical value would be unity.

The parameter B is called the ignition parameter or Frank-Kamenetskii parameter for the system. When known properties and boundary temperatures are supplied to the left-hand side of equation (6), the ignition criterion is simply

$$B \geq 1 \qquad \text{Ignition} \tag{7a}$$

$$B < 1 \qquad \text{No ignition} \tag{7b}$$

This represents the power of the constant reaction rate method. A single figure-of-merit, the ignition parameter, combines information about the reactive surface area, heat transfer resistance including sample dimensions and thermal conductivity, and reaction kinetics parameters.

A typical application is to know specimen size and reactive area. Then, equation (6) may be solved for B = 1 to yield the specimen surface temperature that would cause ignition. Often, reactive area is not known, and equation (6) provides a functional relationship between reactive surface area and the ignition temperature.

The method described above may be extended as follows. For cylindrical geometry, the factor of 2 preceding k is replaced by a factor of 4. When the specimen is irradiated, its volumetric decay power may be taken into account by replacing the boundary temperature T_∞ used for linearization in equations (4), (5), and (6) by a value T_{dk} which is T_∞ augmented by the decay power temperature increase

$$T_{dk} = T_\infty + \frac{Q_{dk} L^2}{2 k} \tag{8}$$

When natural convection heat transfer resistance is comparable to specimen internal heat transfer resistance, the specimen boundary temperature T_i and ambient fluid temperature are related by

$$h \left(T_i - T_\infty \right) = Q_v L \tag{9}$$

and the formula in equation (6) for B is used with an effective thermal conductivity k_e replacing k and given by

$$k_e = k \left[1 + \frac{2 k}{h L} \right]^{-1} \tag{10}$$

Note that thermal radiation from the specimen surface can be comparable to natural convection, so a linearized radiation heat transfer coefficient should be added to h in equation (10). These contingencies cover most situations of interest, where conduction is essentially one-dimensional. For other geometries or for extension to two dimensions, the essential first step is to derive an analytical formula analogous to equation (1) for the system temperature difference. A two-dimensional cylindrical geometry problem of this nature is described in our earlier work [Epstein, et al., 1996] and its simplification via the present method is discussed later.

2.2 Reaction Kinetics

Here we introduce appropriate literature correlations for various gaseous atmospheres, Table 1 and Figure 2. The correlations are presented in consistent units, and all but the McGillivray correlation for non-zero water vapor follow the Arrhenius form required for the use of equation (6). When the water vapor pressure appears in a correlation, the pre-exponential factor in equation (6) is replaced by the table value below and multiplied by the water vapor pressure factor in the table, i.e., k_o is replaced by ($k_o P^n$). The McGillivray correlation for dry air can be used directly in equation (6). For cases with relative humidity between 10% and 90%, the dry McGillivray correlation can be multiplied by a factor that is independent of relative humidity, and ranges from about 2 at 30°C to 8 at 100°C. From the Pearce correlation with variable relative humidity, the pressure is only taken to the 0.3 power, so over this relative humidity range the Pearce

Figure 2:
Comparison of Literature Correlations for U Metal Reactions, Weight Gain kgO$_2$/m^2 · s. Gases are Pure H$_2$O (Pearce oxy-free, + symbol), Air at 100 % Relative Humidity (Pearce 100% RH, solid line), Dry Air (McGillivray dry, xx symbol), and Several Correlations for Air with 75% Relative Humidity (see legend).
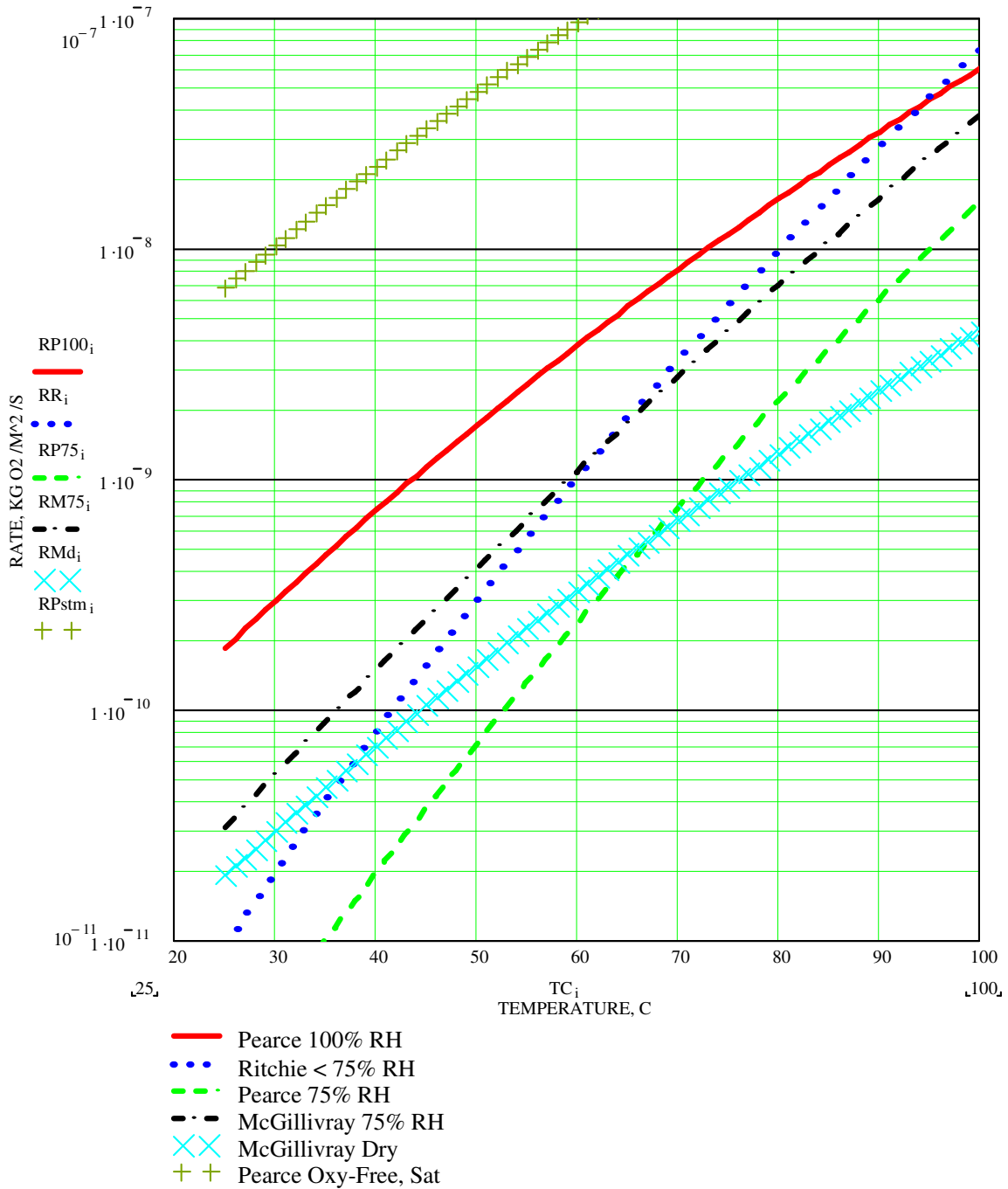
<table>
<tr><td colspan="4">

Table 1:
Literature Correlations for U Metal With Various Gases. In all cases, T is temperature in Kelvins, P is pressure in Kilo Pascals, and the rate is provided in $kgO_2/m^2/s$.

</td></tr>
<tr><td colspan="4">

A.   Correlation following $R = k_o P^n \exp\left(- T_E / T\right)$

</td></tr>
</table>

Correlation	k_o, $(kgO_2/m^2/s)$	T_E, (K)	n
Pearce, Oxygen-Free Water Vapor	0.0594	4937	0.5
Pearce, 100% RH, In Air, T < 100°C	598.0	8589	0
Pearce, < 100% RH, In Air, T < 192°C	$1.023 \cdot 10^5$	11490	0.3
Ritchie, < 75% RH, In Air, T < 100°C	$2.111 \cdot 10^8$	13280	0
McGillivray, Dry Air	10.95	8077	0

B.   McGillivray correlation for U-H$_2$O-Air

$$R = \frac{0.4195\, P \exp\left(\dfrac{-6432}{T}\right)}{1 + 2.48 \times 10^{-7}\, P \exp\left(\dfrac{5327}{T}\right)} + 10.95 \exp\left(\dfrac{-8077}{T}\right) \frac{kg\, O_2}{m^2\; s}$$
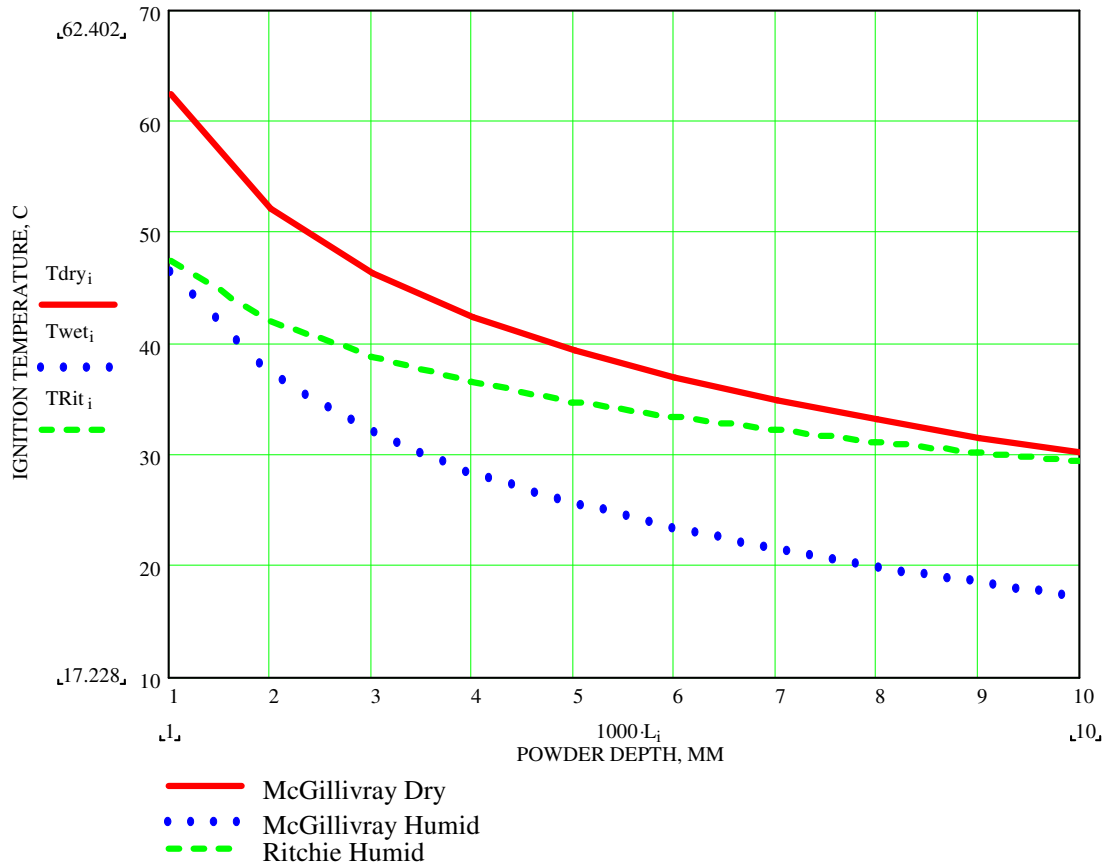
result would only vary by a factor of 2. Note that the Pearce correlation cannot be used for very low relative humidities, for it cannot fall below the dry air value. In the temperature range shown, and for the range of relative humidities mentioned, the effect of water vapor pressure is arguably small, and in fact, Ritchie chose to neglect this variation as seen from the table. The activation energies used by Pearce and Ritchie for moist air are higher than those for 100% humid or dry air; hence, these two curves non-physically cross their limiting cases.

2.3   Example and Uranium Hydride Conclusions

An example for application of the method is to understand observations of uranium hydride powder ignition by [Hartman, et al., 1951]. Such an evaluation was presented in our earlier work [Epstein, et al., 1996] using the exact constant rate solution without the Frank-Kamenetskii approximation, but with a model equation neglecting internal heat transfer resistance, and using the full McGillivray correlation, which cannot be simplified as described above. Here we employ equation (6) directly using the following parameter values: Bed thermal conductivity k = 0.4 W/m/K typical of uranium metal beds, h = 5 W/m^2/K typical of natural convection plus thermal radiation for the temperature range of interest, ϕ = 0.4 porosity typical of a random bed, ΔH = 3.4 x 10^7 J/kgO$_2$ for U oxidation with O$_2$, and d = 1.85 micron particle size per Hartman's distribution. Predicted results are shown in Figure 3 for dry air (McGillivray), humid air using 3 times McGillivray which is typical of 40 - 60°C range (see Figure 2), and humid air using Ritchie which is also independent of relative humidity. Note, the higher activation energy used by Ritchie leads to its result spanning results obtained using McGillivray.

Hartman observed ignition of a sample of 5 grams of uranium hydride powder placed upon a small disc under ambient conditions in his laboratory, presumably within an enclosure. We do not know the temperature or relative humidity, but it is reasonable to assume that the relative humidity in Pittsburgh at the U.S. Bureau of Mines was neither extremely low nor extremely high, and that the McGillivray Humid curve in Figure 3 is a reasonable representation of the kinetic rate law. A sample height of about 7 mm or higher leads to predicted ignition at room temperature, and this is consistent with a disk the size of a dime. The result shown here is very close to our earlier comparison, and from this we conclude that the

Figure 3:
Ambient Temperature, °C, as Function of Powder Depth, mm, for Ignition of Small Deposits of Fine Uranium Metal or Hydride for Various Kinetic Rate Laws, particle diameter 1.85 micron.

reaction kinetics of uranium hydride are for practical purposes well-represented by those for uranium metal.

3.0   PYROPHORICITY INCIDENTS

3.1   Accounts of Incidents

Pyrophoric behavior of metals used in reactors and defense applications, such as uranium, plutonium, zirconium, and hafnium, is documented in available reports and publications dating from the decade of the 1950's. Apparently, most or all of the material was classified. The earliest clear reference on the topic, AEC Uranium Fire Experience [no author name appears, but this report is sometimes associated with the name of the declassifier, Pearson; see References], dates from 1954, and specifically notes at that time,

> *"… perhaps the bulk of the AEC uranium fire experience does not appear to have been recorded and that treatment of the problem to date has been basically confined to uranium fire extinguishment with results that differ with each Operations Office concerned."*

The reference goes on to say,

> *"AEC uranium fires cannot presently be statistically studied due to the absence of recorded information. One contractor (National Lead at Fernald) has experienced upward of 300 such fires in a single month."*

The reference describes select incidents in a few sentences apiece, categorizes incidents by type, briefly describes oxidation phenomena, hypothesizes causes for uranium fires, summarizes current mitigation techniques, and proposes a rather detailed research plan to formally understand causes of uranium fires and preventive measures. Two articles on the industrial hazard of pyrophoric reactor materials appeared in the December 1956 issue of Nucleonics [see References], motivated by several deaths and serious injuries which had occurred that year in separate incidents with zirconium, uranium, and thorium.

Accounts of uranium pyrophoricity during storage and processing have recently been given by Abrefah, et al., [1999] and Demiter as contained in [Plys, et al., 2000]. The surveys cover the period 1955 - 1995 and are essentially updated versions of the much earlier report, AEC Uranium Fire Experience. Douglas United Nuclear (DUN) developed a process for encapsulating metallic uranium scrap in concrete cylinders cast in thin sheet metal cans. A series of tests were performed at DUN to determine the conditions for ignition of the concreted cylinders. The results are reported in Weakley [1980].

As we have already learned, the factors which influence uranium pyrophoricity are metal particle size, ambient temperature, ambient moisture content, and heat sources other than oxidation-kinetic heating. Information on one or more of these factors is missing from the documentation of uranium metal ignition incidents. Consequently it is not possible to provide an unambiguous comparison between ignition theory and ignition incidents. However we can demonstrate that the ignition events are compatible with thermal ignition theory.

3.2   Classification of Incidents

A careful reading of the reviews of uranium fire or explosion incidents [Pearson, 1954; Abrefah, et al., 1999; and work by J. Demiter presented in Plys, et al., 2000] indicate that the uranium metal ignitions at manufacturing or government sites can be categorized into the following four types:

(1)   Onset (ignition) of a chemical runaway reaction inside opened drums containing clad uranium fuel elements with exposed uranium surfaces (due to corrosion or sectioning) or uranium scrap consisting of lathe turnings and saw fines. Also ignition of uranium scrap encapsulated in concrete. High ambient temperature and humidity were presumed to be responsible for these ignitions. The runaway ignitions inside drums or concrete cylinders were followed by slow burning similar to a charcoal fire.

(2)   Explosions inside drums containing corroded fuel elements or metal scrap. An explosion occurred while the drum was being tapped to loosen the lid and at the instant that ambient air entered the drum. Apparently hydrogen gas was also present in the drums that exploded.

(3) Ignition of highly corroded fuel elements or defueled, highly porous cladding following accidental dropping onto the floor or during element-to-element contacting under violent shaking conditions in fuel dissolvers or while in transfer trays.

(4) Ignition of badly corroded or powdered uranium metal in air at ambient temperature or ignition of accumulated metal powder under water.

Unfortunately, a convincing explanation could not be made for observations of ignition by impact under water, and these are not pursued here.

3.3   Ignition of Uranium Scrap in Drum Storage

Thousands of spontaneous fires have been experienced at room temperature during drum storage of lathe turnings or uranium briquettes made from compacted turnings [Pearson, 1954]. An appropriate ignition model for these fire experiences is a packed bed of uranium pieces of a given porosity ϕ and specific area A / V which fills an upright cylindrical drum of radius R and height L. This is modeled using the heat conduction equation written in cylindrical coordinates with a volumetric heat generation term from the oxidation reaction, and a convective boundary condition is applied to the cylinder top, side, and bottom. An exact solution to this equation for the case of distinct heat transfer coefficients for the three surfaces is provided in [Epstein, et al., 1996] in terms of an infinite series, and in this work the heat generation term was exactly found. However, by applying the Frank-Kamenetskii approximation, the otherwise daunting expression in the reference becomes tractable, as shown here.

The solution for the maximum temperature difference may be written as

$$T_{max} - T_{\infty} \;=\; \frac{A_v \, f \, L^2 \, \Delta H \, C \, e^{-\,T_E/T}}{2 \, k_b} \tag{11}$$

$$f \;=\; \frac{2 \, L_o}{L^2}\left(B_d \, \frac{z_m}{L} + 1\right) - \left(\frac{z_m}{L}\right)^2 - \frac{B_s}{L^3} \sum_{n=1}^{\infty} C_n \left[\cos\left(\alpha_n \, z_m\right) + \frac{B_d}{\alpha_n \, L} \sin\left(\alpha_n \, z_m\right)\right] \tag{12}$$

where a form factor "f" is introduced which depends upon a ratio of heat transfer coefficients and bed conductivity L_o, Biot numbers B_d, B_s, and B_u, and coefficients of the infinite series C_n, and α_n defined in the reference. The axial location of the maximum temperature z_m must be found by setting (d f / d z_m) = 0. Due to the form of equation (11) it immediately follows that the formula in equation (6) for the ignition parameter can be used if the cylinder height is identified as L, and L^2 is replaced by the product f L^2. The form factor has been evaluated for cases pertinent to typical drum storage in air and is shown in Figures 4a and 4b for cases of an isolated drum and side-by-side drums, respectively. In each case, the upward heat transfer coefficient is 10 W/m^2/K and the downward heat transfer coefficient is 1 W/m^2/K (nearly insulated, small downward conduction loss). An isolated drum has free convection on its side, hence h = 10, while side-by-side drums radiate to one another and have lower natural convection, hence h = 1 is used to distinguish these cases. Values of the form factor are given in each figure for decreasing values of R / L, and note that for R / L greater than about 3, the value is nearly independent of the ratio because conduction is nearly all axial. Note the range of R / L is varied from flat pancake through a tall cylinder.

9

Figure 4a:
Values of Geometric Form Factor "f" of Equation (12) for Various Canister Radii R and Aspect Ratios R / L, Isolated Scrap Drums.
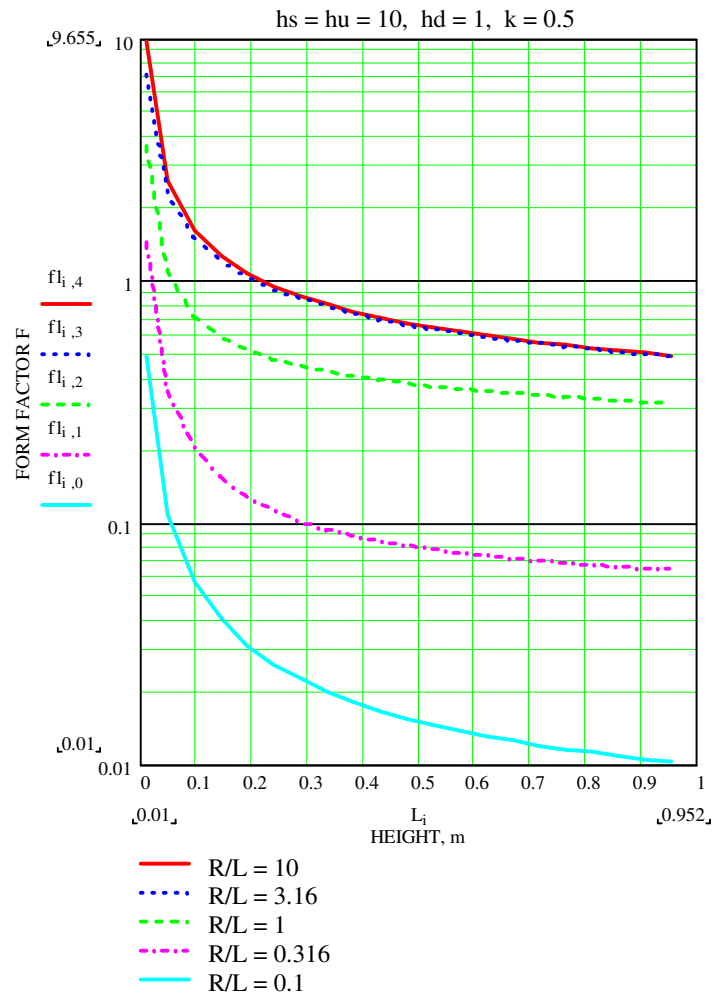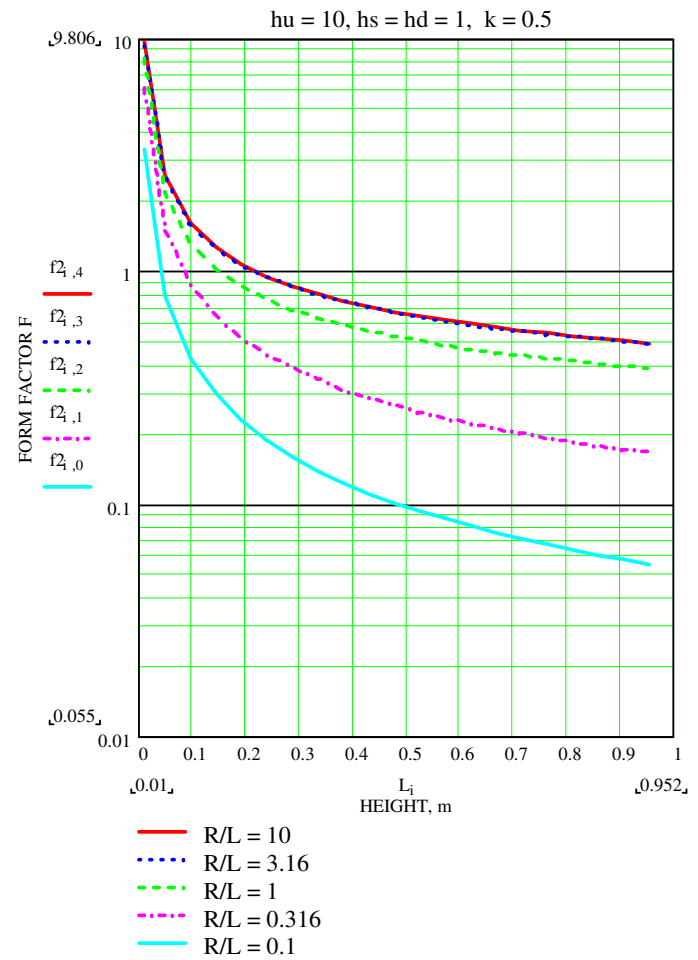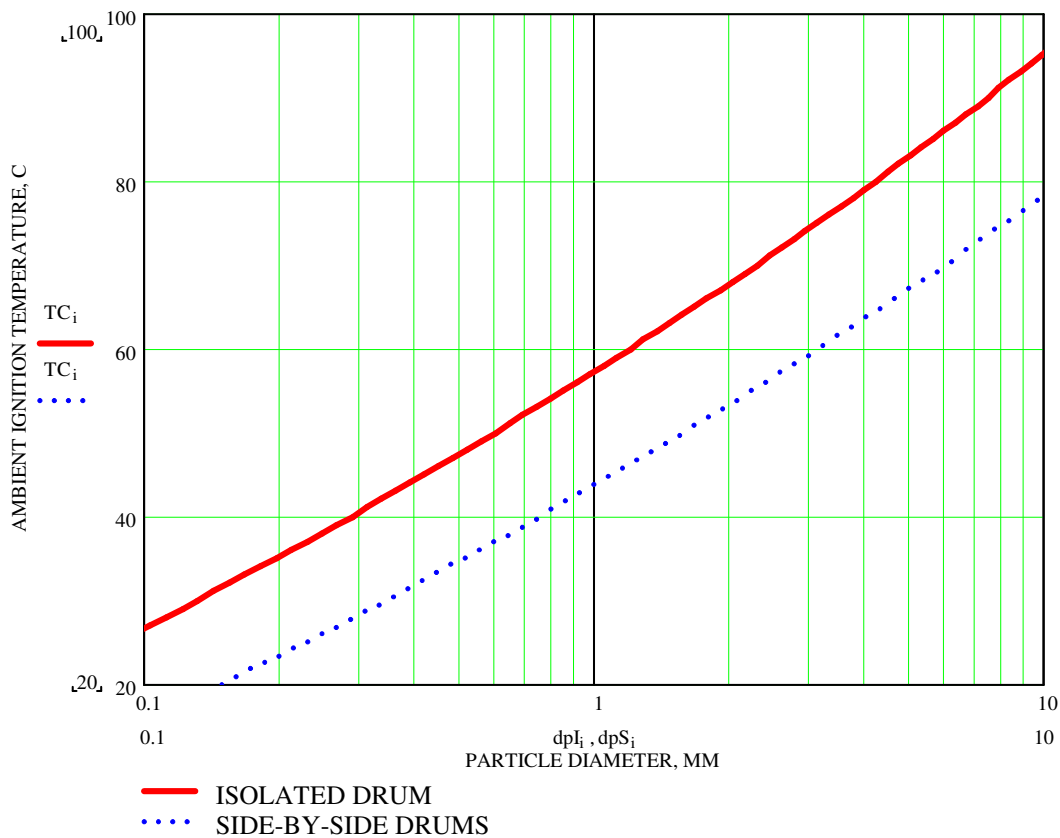
Figure 4b:
Values of Geometric Form Factor "f" of Equation (12) for Various Canister Radii R and Aspect Ratios R / L, Side-by-Side Scrap Drums.

Figure 4a: hs = hu = 10, hd = 1, k = 0.5

R/L = 10
R/L = 3.16
R/L = 1
R/L = 0.316
R/L = 0.1

Figure 4b: hu = 10, hs = hd = 1, k = 0.5

R/L = 10
R/L = 3.16
R/L = 1
R/L = 0.316
R/L = 0.1

For a 50 gallon drum, appropriate values are R = 0.29 m and L = 0.89 m. From Figures 4a and 4b, the form factor for an isolated drum is f = 0.065 and that for side-by-side drums is 0.17. A scrap porosity of $\phi = 0.4$ and thermal conductivity of 0.5 W/m/K (consistent with the form factor figure) are used with the McGillivray dry kinetics multiplied by a factor $\xi = 3$ to account for typical humidity. This is all the information required to use equation (6) to calculate the relationship between effective scrap particle size and ambient ignition temperature, shown in Figure 5. These results are nearly the same as those in our earlier work, but are obtained expeditiously through the form factors above and the simple ignition criterion of equation (6) (Note previous results were published in terms of A / V, and the effective particle size shown here is somewhat more intuitive to understand). The information provided here is useful for many practical situations.

Figure 5:
Ambient Temperature for Ignition of Isolated (solid) and Side-by-Side (dash) 50 Gallon Drums with Uranium Metal Scrap for Various Average Scrap Sizes, mm.

3.4   Spontaneous Ignition of Porous or Finely Divided Uranium

Another common experience is the ignition of porous or powdered uranium metal or metal chips in air after resting uneventfully for several days in an open container. One incident occurred under water. Powder gradually accumulated in a sump under about 25 feet of water. Approximately once a month the powder reacted violently and produced a 30-ft high geyser in the sump. After each event, the sump was

cleaned and new powder would accumulate. Obviously, the ignition event required a critical volume of powder. This critical volume is easily understood in terms of thermal ignition theory. A gradual increase in volume will eventually result in an unstable situation in which the reaction power production exceeds the heat loss rate from the powder. Our past work has demonstrated that thermal ignition theory is capable of predicting ignitions of uranium metal powder under well-controlled laboratory conditions. It stands to reason, then, that all the reported incidents of spontaneous ignition of powdered uranium material (or chips) were classical chemical runaway events that could readily be rationalized by thermal ignition theory if the important parameters were known (particle size, volume of powder, ambient temperature and humidity, etc.). Methods described above will be used later in this paper to show how gradually collected uranium fines can ignite in this manner, even under water.

3.5   Explosions of Storage Drums

Explosions of storage drums have been observed when fuel or scrap is found to be severely corroding in their containers. In many reported incidents, flashing of the fuel or explosions occurred when the containers were opened. The flashing was believed to be the spontaneous ignition of uranium or uranium hydride powder which became suspended due to the mechanical disturbance of opening the container. Suspended uranium powder could also be the cause of the explosions that were reported. Such explosions are known as dust explosions. It is well known that if a settled dust is disturbed, a dust suspension may be formed and ignited by, say, a spark. Hydrogen gas is usually present inside the containers that store corroded fuel, and this will exacerbate the situation because ignition requirements are reduced for combined flammable gas and dust mixtures in air.

Metal dust is quite flammable and explosive. Depending on the dust concentration, the flame speed may be high and comparable with that in gas deflagrations. The hazard of an uranium dust explosion upon opening a container storing corroded fuel is about the same as a hydrogen explosion. This can be demonstrated through knowledge of the important explosibility characteristics of uranium dust suspensions, namely, the minimum explosive concentration and the minimum ignition energy. This information is apparently not available for uranium metal dust. However, the information can be obtained by appealing to classical thermal ignition theory.

A transient version of ignition theory was used for analysis of this problem in order to quantify the effect of an initial spark creating a hot spot, to observe if a combustion front would propagate or die out. The theory is not presented here in detail because it departs from the main technique that is the subject of this paper, but it is described in our full work.

We have found the lower concentration limit for uranium dust to be about 0.19 mg/cc, which requires a large spark initiator, and is in good agreement with other metal dusts. For a typical spark energy encountered in practice, on the order 10 to 40 mJ, the corresponding concentration that can sustain a dust explosion is around 0.5 to 0.6 mg/cc. Spark energies approaching a minimum ignition energy (MIE) of 0.15 mJ are sufficient at stoichiometric concentration.

From these findings, we conclude that the presence of combined hydrogen gas and suspended metal or hydride dust due to container handling are sufficient to explain this category of experiences.

4.0   DETERMINISTIC APPLICATION

A useful application of the methods above is identification of a simple criterion for screening pyrophoricity potential, with various formulas depending upon the geometry. As an example, we can plot

the tradeoff between allowable particle size and metal content, and create a family of curves as other parameters such as the ambient temperature, thermal conductivity, or container size are varied. This allows the safety of storage or transportation to be easily screened.

We mentioned above that ignition has been observed in situations where material appears to benignly accumulate over a period of time, even under water. Here, a realistic example is given for accumulation of uranium particulate in an under water container as chips and sludge are stored in a water treatment system during remediation operations. Ignition is possible when accumulation causes the reactive surface area to increase faster than particle oxidation causes it to decrease, and there is significant heat transfer resistance in the accumulating particulate. For this example, a mixture of metals and oxides is accumulated in a 16-inch (40-cm) diameter container convecting to basin water at 15°C. Decay power is neglected. A typical submerged heat transfer coefficient is about 150 $W/m^2/K$, and values of the geometric form factor "f" of equation (12) required for submerged storage are given in Figure 6a. Appropriate values to employ within the debris are k = 3 W/m/K and $\phi = 0.4$. The pertinent reaction rate is the oxygen-free U-H_2O reaction rate because the large particle area will soon scavenge dissolved oxygen in the debris, and a safety factor of $\xi = 3$ is applied to the kinetic rate law for screening the safety issue.

The actual average particle size of metallic debris is not known a priori, nor is the volume fraction of metal (the remainder being oxide) known, although reasonable values for these can be established by experience. Therefore the tradeoff between allowable metal volume fraction, effective metal particle size, and debris height can be examined directly through equation (6) using form factors from Figure 6a. As debris accumulates to depths of 10, 20, 30, and 40 cm, form factors are 1.3, 0.8, 0.5, and 0.4, respectively. Results of the analysis are shown in Figure 6b. Safe combinations of metal volume fraction and particle size lie below and to the right of each line for a given depth of debris, and unsafe combinations lie above and to the left. Imagine that the true metal fraction of debris is 40% by volume, and that the average particle size is 1 mm. If the maximum allowed debris depth is 40 cm, then the operation is always safe (coordinates 1 mm, 0.4 fraction are below the 40 cm deep curve). However, if the metal volume fraction actually accumulated during operations is closer to 80%, then operations would be safe until waste accumulated to just about 30 cm in depth. Thereafter, the potential for thermal runaway exists.

The method described here, coupled with the values for the form factor f or suitable use of equation (6), can be applied to screen a variety of practical applications. Examples evaluated to date include:

- Ignition of isolated scrap pieces with significant cracking and internal hydriding,

- Ignition of metallic fuel elements damaged at one end which lacks cladding and whose exposed metal is cracked with internal hydride, or elements with axial tears in cladding; these become fin problems where the undamaged element length is available for heat rejection,

- Ignition of an array of metallic fuel elements damaged as described above; here heat loss was essentially radial and the element array was treated as a distributed medium with thermal conductivity accounting for inter-element thermal radiation,

- Ignition of a basket of scrap pieces damaged as described above, also treated as a distributed medium with radial heat loss,

Figure 6a:
Values of Geometric Form Factors "f" of Equation (12) for Various Canister Radii R and Aspect Ratios R / L, Under Water Storage Convecting Sideward and Upward, Insulated Bottom.
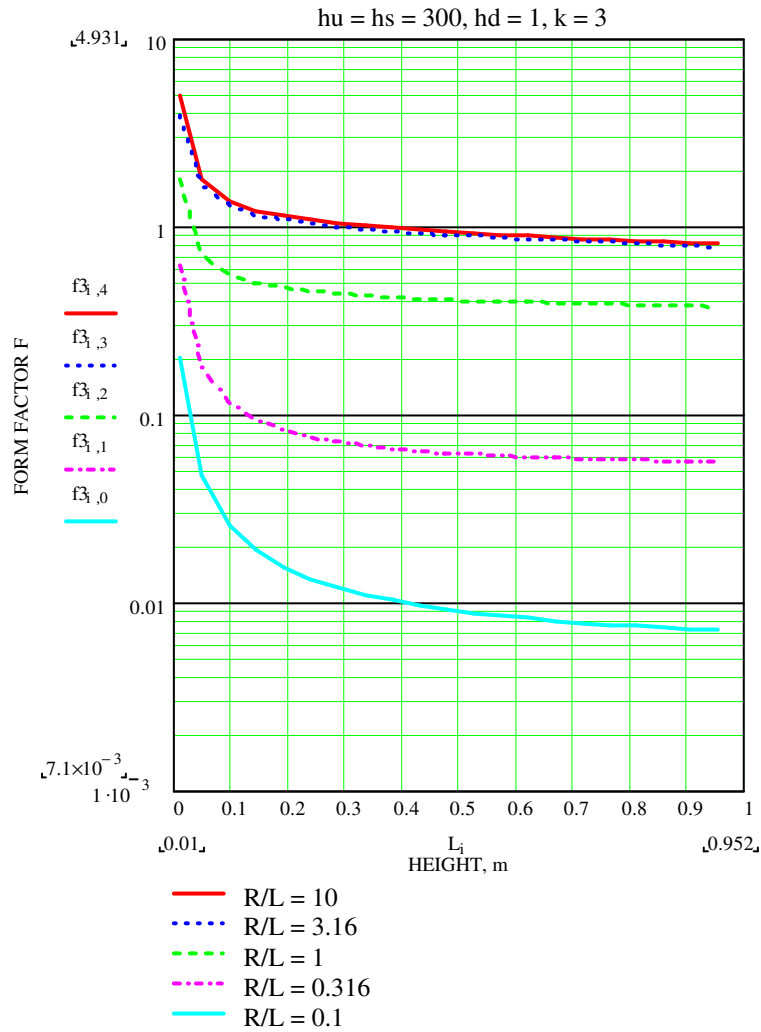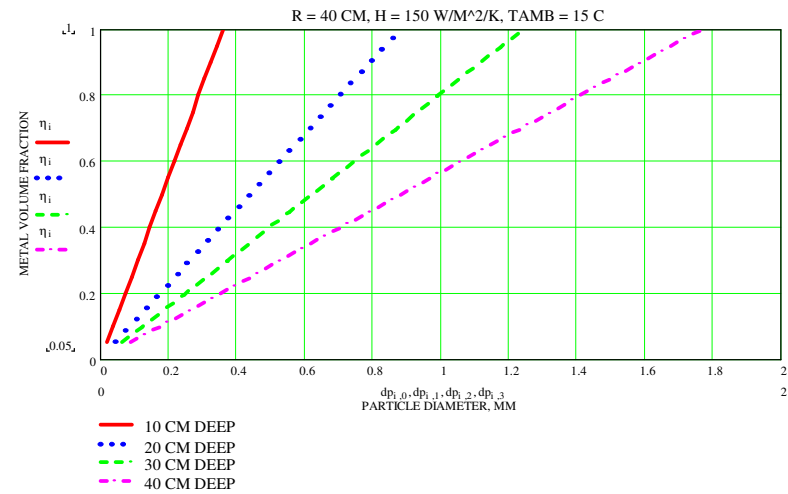
Fig. 6b:
Ignition Threshold Combinations of Metal Volume Fraction and Particle Diameter, mm, for Under Water Storage of Uranium Fines in a 16" (40 cm) Diameter Container, as Fines are Accumulated to Various Depths. Safe combinations lie below the curves, unsafe combinations lie above the curves.

14

- Ignition of a basket of damaged scrap pieces designed with radial copper fins to provide a conduction path from the center to periphery, and

- Ignition of collected fine chips and metal-bearing sludge in under water storage.

In all cases, appropriate expressions for the maximum temperature difference were obtained and used to modify the conductivity or apply a form factor in equation (6), as shown in the examples above. These analyses allowed rapid screening of metal fuel processing safety for a variety of gaseous atmospheres, normal and off-normal conditions, and fuel damage states, and provided technical bases for process design, including for example, the acquisition of copper scrap baskets.

5.0   PROBABILISTIC APPLICATION

Simplicity of the ignition criterion in equation (6) facilitates uncertainty analysis and probabilistic application of the method. For example, the range of reaction rate data manifest in the differences between correlations shown in Figure 2 implies the need for prudent examination of rate law uncertainty. Particle roughness also contributes to enhanced surface area, and hence, reaction rates. A safety factor ξ is usually applied to the pre-exponential factor k_o in equation (6) to formally indicate uncertainty, and the effect of uncertainty in the activation energy is usually subsumed in this pre-exponential factor. For a collection of scrap pieces or particles, the thermal conductivity and porosity are the next two parameters that are important for uncertainty.
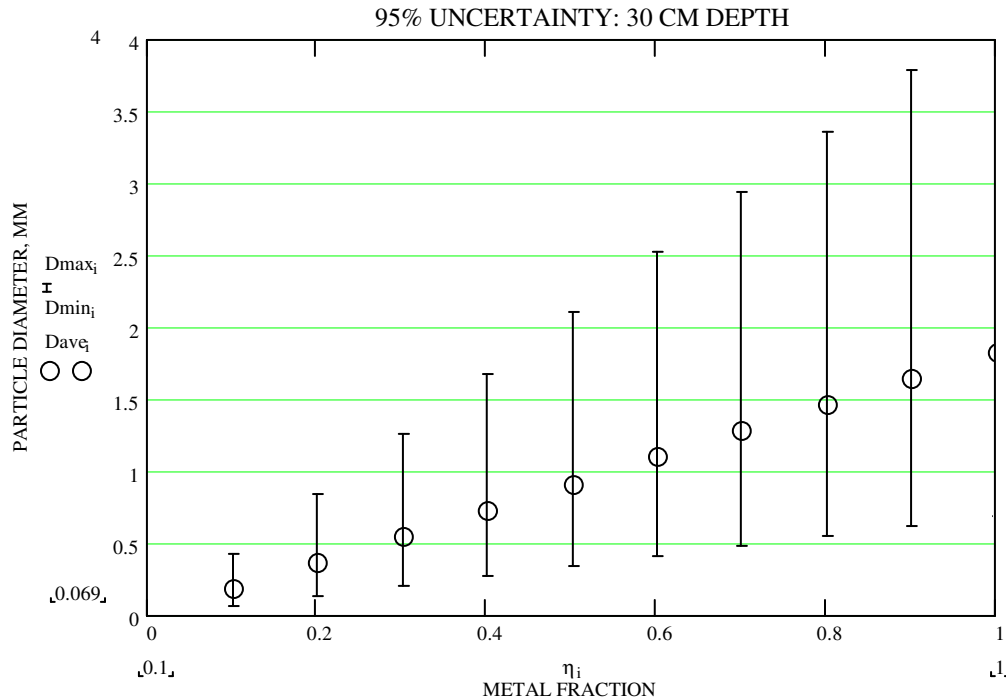
Consider under water accumulation of fine particulate and sludge as in the previous example, but with variation in these parameters as follows: $1 < \xi < 10$, $2 < k < 3$, and $0.3 < \phi < 0.5$, for an accumulated depth of 30 cm which was judged safe for central estimates when in true operation the metal fraction was 50% and the particle size was 1 mm. Figure 7 shows the 95% uncertainty bandwidth and median estimates for this case using error bars on the particle size for a given metal fraction; safe cases now lie above and to the left of the uncertainty band. The uncertainty bandwidth increases with metal fraction because of the Arrhenius rate law, and for the case of 1-mm particles, a metal fraction of less than about 25% is safe, or half the value obtained through the deterministic analysis.

Probabilistic evaluations of ignition potential were made for Hanford SNF process safety assessment early in the design process, and an example is documented in [Plys, et al., 2000]. This evaluation supported the copper scrap basket design, because for the baseline design, the probability of ignition was low for normal conditions, but not acceptable for off-normal conditions. A similar probabilistic evaluation was used to understand differences between French fuel which had experienced under water ignition upon impact and the fuel presently stored in the Hanford K basins. Nominal parameter values and ranges for the both fuel types could be assigned by judgement, and ignition potential was evaluated by calculating resulting distributions for the value of the ignition parameter B in equation (6). The French fuel had about a 0.5% chance of exceeding B = 1, while the value for K basins fuel was well below 10^{-6}. The point of the comparison is that we could not exactly know the property values to assign to those fuel elements observed to ignite under water, but the ignition parameter provides a single figure-of-merit to compare relative similarity or difference between two situations.

6.0   TRANSIENT APPLICATION

Previous examples have presumed accumulation or assembly of sufficient reactive material to cause ignition, without considering that the time for assembly, or the time to achieve steady-state

Figure 7:
Uncertainty Range for Combinations of Debris Metal Fraction and Average Metal Particle Diameter that could Lead to Ignition when Rate Law Uncertainty, Thermal Conductivity, and Bed Porosity are Varied.

conditions, would be sufficient to change assumed initial conditions. The rate laws summarized in Table 1 define linear change in particle radius with respect to time, and a shrinking core model implies surface area decrease with the square of time. So if small particles are accumulated over a sufficiently long period of time, the particle size distribution can evolve into a steady state with an asymptotic reacting area.

Consider accumulation of particles in a settler whose length is much greater than its radius. If the characteristic time for accumulation is on the order of one year and the basin temperature is 15°C, particles smaller than about 0.25 mm diameter should be completely reacted over this time scale, assuming oxygen depletion in the reacting particle bed so that the oxygen-free rate law applies. Heat transfer resistance is very small when particles begin to accumulate, and increases to a limiting value used for a cylindrical steady-state evaluation when the settler is full. The time scale for heat conduction is much faster than that for particle accumulation, so the temperature distribution may always be regarded as steady-state. The characteristic distance for conduction varies between half the bed height for a shallow layer of particles, to about 2/3 the radius to match transient results for a full settler using a lumped parameter model.

The evolution of the particle size distribution is given by a simplified form of the traffic equation where the corrosion velocity is constant for all particle sizes [Plys and Malinovic, 1999]:

$$\frac{\partial n(r,t)}{\partial t} = S(r) + U(t) \frac{\partial n(r,t)}{\partial r} \tag{13}$$

$$U = \frac{238}{32} \frac{\dot{m}''_{ox}(T)}{\rho_m} \tag{14}$$

where $n(r,t)$ =   Number of particles of size range within dr of r,
$\qquad$ $S(r)$ =   Source rate (constant with time),
$\qquad$ $U(t)$ =   Corrosion velocity, m/s,
$\qquad$ $\dot{m}''_{ox}(T)$ =   Reaction rate, $kgO_2/m^2/s$, and
$\qquad$ ρ_m =   Metal density, kg/m^3.

An effective numerical approach is to apply the sectional method and write a mass balance for "bins" of defined radius range. Properties associated with bins are:

$\qquad$ N_i =   Number of particles in bin i,
$\qquad$ Δr_i =   Size range of bin i,
$\qquad$ S_i =   Source rate to bin i,
$\qquad$ r_i = $\sqrt{r_{\ell i}\, r_{h i}}$, = Average radius of bin i,
$\qquad$ A_i = $4\pi r_i^2$, = Reactive surface area of a single particle,
$\qquad$ V_i = $\frac{4}{3}\pi r_i^3$, = Volume of a particle in bin i, and
$\qquad$ $r_{\ell i}, r_{h i}$ =   Low and high radii of bin i.

Particles in a bin react to produce oxide, decrease in size, and eventually move to the next lower radius bin. The metal source to a bin is given by

$$S_i = \rho_m \eta \dot{V} s_i \tag{15}$$

where $\dot{V}$ =   Volumetric rate of material addition, m^3/s,
$\qquad$ s_i =   Incoming particle distribution, number per unit bin volume, $\# / m^3$,
$\qquad$ ρ_m =   Metal density, kg/m^3, and
$\qquad$ η =   Metal volume fraction.

Hence, the overall particle balance for bin i is:

$$\frac{d N_i}{dt} = S_i + U\left[\lambda_{i+1} N_{i+1} - \lambda_i N_i\right] \tag{16}$$

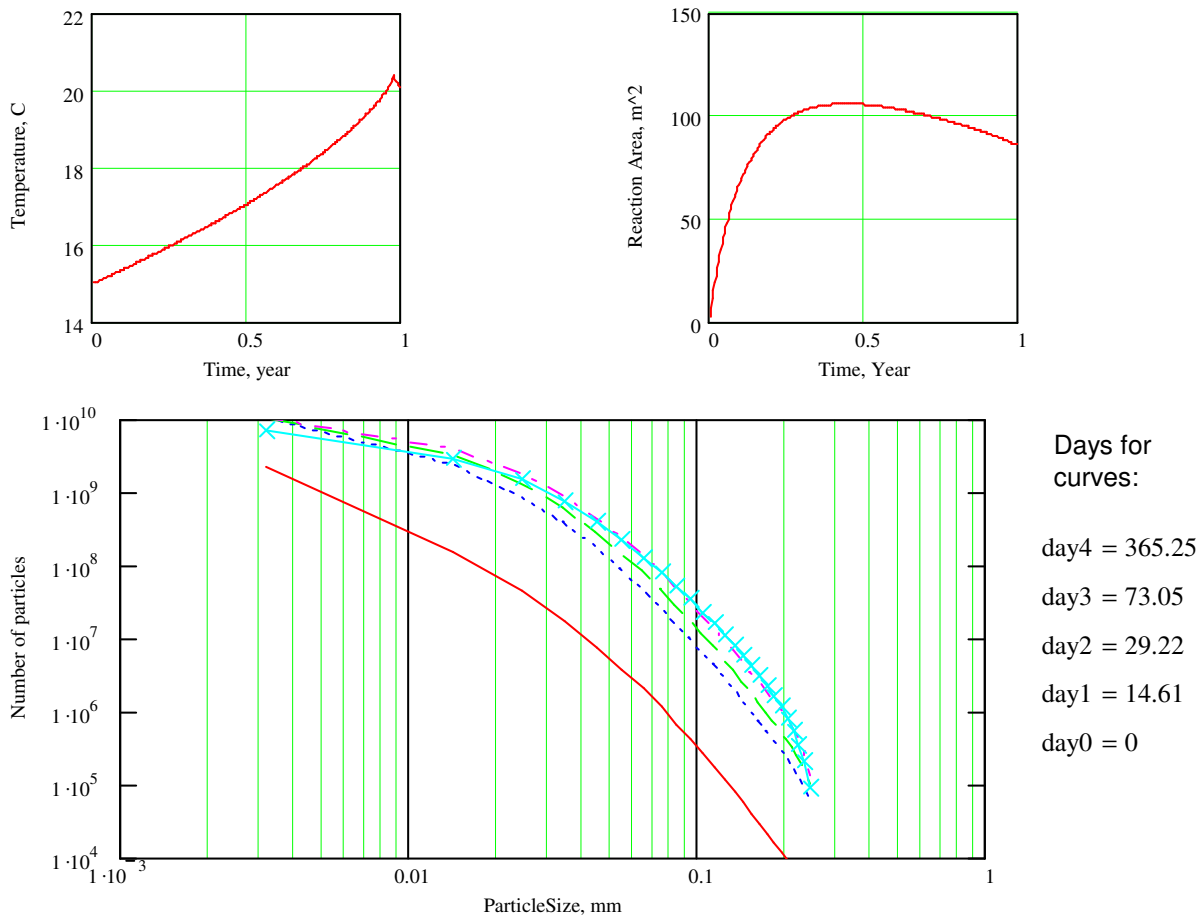where $\lambda_i \equiv -\dfrac{A_i}{V_i - V_{i-1}}$ $\qquad\qquad\qquad$ (17)

A single mass balance is written for oxide accumulated in the settler considering material addition source and transformation of metal particles to oxide. At any time, the total reactive area and volume of

the metal are found by integrating over the metal particle distribution. Then, the ignition parameter from equation (6) can be directly evaluated, and if it is less than unity, the temperature can be found from equation (6) as well. Note that the constant reaction rate assumption which underlies equation (6) is consistent with the assumption implicit in the particle size evolution equation; an exact solution would require a separate particle size distribution and temperature to be tracked as a function of position.

An example transient calculation is shown in Figure 8 for a case where the incoming particle size distribution is log-normal with a mean of 100 µm and a standard deviation of 100 µm, the metal volume fraction is 50%, and a rate law multiplier $\xi = 3$ is used for safety. The reactive area reaches a maximum of just over 100 m^2 after about 1/4 year, and the particle size distribution reaches an asymptotic shape after only about one month. In a complete analysis, it was shown that these conclusions were robust with respect to the incoming particle size distribution and metal volume fraction.

Figure 8:
Example Settler Transient Calculation: Temperature and Reactive Surface Area History (top), Particle Size Distribution History (bottom).

Temperature and reactive area: Discontinuity in T when height = 2/3 diameter

Days for curves:

day4 = 365.25

day3 = 73.05

day2 = 29.22

day1 = 14.61

day0 = 0

Particle size distributions for increasing times from lower (solid) to upper (crosses) curves

Transient calculations may also be useful in cases where system heat capacity is large or in which the boundary conditions vary significantly over time. An important caveat however is that it is difficult to defend a safety case on the basis of time to thermal runaway, because uncertainty in the kinetic rate law and heat transfer resistance lead to significant uncertainty in the transient temperature history for a case that is unstable in the steady-state.

7.0   REFERENCES

Abrefah, J., et al., 1999, "Analysis of Ignition Testing on K-West Basin Fuel," PNNL-11816, UC-602, Pacific Northwest National Laboratory, Richland, WA, August.

Epstein, M., et al., 1996, "On the Prediction of Ignition Potential of Uranium Metal and Hydride," Nuclear Safety, Vol. 37, pp. 12-26.

Frank-Kamenetskii, D.A., 1969, "Diffusion and Heat Transfer in Chemical Kinetics," Plenum Press, NY.

Hartman, et al., 1951, "The Explosive Characteristics of Titanium, Zirconium, Thorium, Uranium, and their Hydrides," U.S. Bureau of Mines, Report of Investigation 4835, U.S. Dept. of Interior, December.

McGillivray, G. W., et al. 1994, "Studies of the Kinetics and Mechanism of the Oxidation of Uranium by Dry and Moist Air - A Model for Determining the Oxidation Rate Over a Wide Range of Temperatures and Water Vapor Pressures," Journal of Nuclear Materials, 208, pp. 81-97.

Nucleonics, 1956, "Pyrophoricity - A Technical Mystery Under Vigorous Attack," Smith, R.B., Vol. 14, No. 12, pp. 28-33, December; and "The Public and Nuclear Risk: Lessons Learned from a Pyrophoricity Incident," Interview with Merril Eisenbud, Vol. 14, No. 12, pp. 34-36, December.

Pearce, R.J., 1989, "A Review of the Rates of Reaction of Unirradiated Uranium in Gaseous Atmospheres," CEGB Report RD/B/6231/R89, Central Electricity Generating Board, Berkeley Nuclear Laboratories, UK.

Pearson, H. E., 1954, "1954 - AEC Uranium Fire Experience," HAN-64841, Hanford, Richland, WA, September 17.

Plys, et al., 2000, "Uranium Pyrophoricity Phenomena and Prediction," SNF-5373, Fluor Hanford Inc., Richland, WA, to be released.

Plys, M.G., and Malinovic, B., 1999, "IWTS Metal-Water Reaction Rate Evaluation," FAI/99-26, Fauske & Associates, Inc., Burr Ridge, IL, March.

Ritchie, A.G., 1981, "A Review of the Rates of Reaction of Uranium with Oxygen and Water Vapour at Temperatures Up to 300°C," J. Nuclear Materials, Vol. 102, North Holland Publishing Co., pp. 170-182.

Thomas, P.H., and Bowes, P.C., 1961, "Thermal Ignition in a Slab with One Face at a Constant High Temperature," Trans. Faraday Soc., Vol. 57, pp. 2007-2017.

Weakley, E. A., 1980, "Interim Report on Concreted Uranium Fines and Chips Billet Curing Tests - A Basis for Resuming Shipment of Concreted Uranium Scrap Billets," UNI-1454, United Nuclear Industries, Inc., May.